

Introduction to Electrostatics in Soft and Biological Matter

David Andelman

School of Physics & Astronomy
Raymond & Beverly Faculty of Exact Sciences
Tel Aviv University
Ramat Aviv 69978, Tel Aviv, Israel

Date: Nov 23, 2004

1 Introduction

It is hard to overestimate the importance of electrostatic interactions associated with charged objects in soft and biological matter. In aqueous environment, typical to many of these systems, charges tend to dissociate and affect a wealth of functional, structural and dynamical properties. Without attempting to enumerate an exhaustive list, we mention a few examples. Polymers are flexible and elongated one-dimensional objects (see, *e.g.*, chapters by Warren, Podgornik, Mackintosh, Bensimon). In aqueous solutions they often carry charges, like the naturally occurring DNA or synthetic polyelectrolytes such as polystyrene sulfonate. The charges on the polymer chain and the counter-ions in solutions have an important effect on the rigidity of such chains and on inter- and intra-chain interactions leading to interesting phenomena of aggregation and condensation, as is seen most often in presence of multivalent counter-ions. The process describing how polyelectrolytes chains migrate in external electric fields is called electrophoresis and is another important phenomena with many applications. Other charged structures are biological cell membranes (see, *e.g.*, chapters by Kozlov and Olmsted). These soft and fluctuating two-dimensional objects are naturally built out of mixtures of charged and non-charged phospholipids. Finally, we mention globular proteins with charge groups on their surface (chapter by Elber), self-assembly micelles made of charged amphiphiles (chapter by Olmsted) and charged colloidal particles (chapter by Frenkel) where the charges play a role in the stabilization of colloidal suspensions.

When will the electrostatic interactions influence the structural properties of soft materials? For soft materials the thermal energy $k_{\text{B}}T$ is comparable to the typical energy associated with deformations and structural degrees of freedom. Another way of saying the same is to introduce a length for which the thermal energy is equal to the Coulombic energy between two unit charges. This is the so-called *Bjerrum length*

$$l_{\text{B}} = \frac{e^2}{\varepsilon k_{\text{B}}T} \quad , \quad (1)$$

which is equal to about 7\AA for room temperature, $T = 300\text{ K}$ and for dielectric constant of water $\varepsilon = 80$. An important concept introduced by Debye and Hückel (1923) is the screening of the electrostatic interaction between two charges by the presence of all other cations and anions in the solution. This will be further discussed below.

In this chapter we will briefly review some of the most fundamental concepts related to electrostatic interactions in soft and biological matter. As this is a vast topic, we will restrict the discussion only to static properties of systems in thermodynamic equilibrium excluding the interesting phenomena of dynamical fluctuations and dynamical responses to external fields. Most of the discussion will be restricted to a mean-field approximation of the electric double-layer problem and the solutions of the classical Poisson-Boltzmann equation. Various effects of fluctuations and correlations will only be briefly mentioned toward the end of the present chapter. An excellent reference for the electric double layer is the classical book of Verwey and Overbeek (1948) which explains the DLVO (Deryagin-Landau-Verwey-Overbeek) theory for stabilization of charged colloidal systems. More recent treatments can be found in many books on colloidal science and interfacial phenomena. For example, Evans and Wennerstöm (1994), Israelachvili (1992), and in a review by the present author Andelman (1995). The topic of polyelectrolytes is briefly treated in most polymer books (e.g., De Gennes (1979)), while the classical (and somewhat outdated) book is by Oosawa (1971). For a more recent review on charged polymers, see Netz and Andelman (2003) and references therein.

2 The Poisson Boltzmann Theory

We will now present the derivation of the Poisson-Boltzmann (PB) theory for ionic solutions. As a mean-field theory, the PB theory relies on the following assumptions: i) the only interactions to be considered are Coulombic interactions between charged bodies. ii) Permanent and induced dipole-dipole interactions are neglected. iii) The charges are taken as point-like objects neglecting any finite size effect and any short-range non-electrostatic interactions. iv) The aqueous solution is modelled as a continuous media with a dielectric constant ε . For water, the dielectric constant is taken to be $\varepsilon = 80$. v) The electrostatic potential $\phi(\mathbf{r})$ that each ion sees is a continuous function which depends in a mean-field way on all the other ions. The charge density profile of all ions $\rho(\mathbf{r})$ is also a mean-field continuous function of the position \mathbf{r} .

It is possible to derive the PB equation starting from a field theory and to obtain the PB equation as a first-order term in a systematic expansion Borukhov *et al* (1998, 2000), Netz and Orland (2000), Burak *et al* (2004a). We will use here a simpler and more heuristic approach. Consider an ionic solution with two ionic species having positive

and negative charge densities (per unit volume) of ρ_+ and ρ_- , respectively. The total charge density at each point is $\rho = \rho_+ + \rho_-$. Defining n_{\pm} as the number density (per unit volume) of the two species, then $\rho_{\pm}(\mathbf{r}) = ez_{\pm}n_{\pm}(\mathbf{r})$, where $z_+ > 0$ is the valency of the cations and $z_- < 0$ of the anions.

The ions are assumed to be mobile and in thermodynamic equilibrium. They will adjust to the presence of some fixed electrostatic boundary conditions, which can be either a constant surface potential (*Dirichlet* boundary condition) or a constant surface charge density (*Neumann* boundary condition). At any point \mathbf{r} , the relation between the potential ϕ and the charge density ρ is given in terms of the Poisson equation:

$$\nabla^2 \phi = -\frac{4\pi}{\epsilon} \rho(\mathbf{r}) = -\frac{4\pi e}{\epsilon} [z_+ n_+(\mathbf{r}) + z_- n_-(\mathbf{r})] \quad . \quad (2)$$

Note that cgs (Gaussian) electrostatic units are used throughout this chapter. However, by using dimensionless energy units and expressing all lengths in terms of the Bjerrum length l_B and the Debye-Hückel screening length (introduced below), the results can be made independent of any specific system of units. Using the above equation one can deduce the electrostatic potential for a *given* ionic distribution. However, in the liquid solution the ions are mobile and will adjust their position according to the local potential they feel. As each ionic species is in thermodynamic equilibrium, its corresponding density has a Boltzmann distribution

$$n_{\pm} = n_{\pm}^0 e^{-ez_{\pm}\phi/k_B T} \quad , \quad (3)$$

where n_i^0 is the reference density of i^{th} species ($i = \pm$) taken at zero potential, $\phi \rightarrow 0$. Substituting eq. (3) into eq. (2), we get the Poisson-Boltzmann (PB) equation for the potential ϕ :

$$\nabla^2 \phi(\mathbf{r}) = -\sum_{i=\pm} \frac{4\pi e n_i^0 z_i}{\epsilon} e^{-ez_i \phi(\mathbf{r})/k_B T} \quad . \quad (4)$$

Alternatively, the PB equation (4) can be derived by requiring that the electrochemical potential μ_{\pm} for the two ionic species is a constant throughout the system

$$\mu_{\pm} = ez_{\pm}\phi + k_B T \ln(n_{\pm}) = \text{constant} \quad . \quad (5)$$

The PB equation is a very useful analytical approximation with many applications. Because the equation is non-linear, it has closed-form analytical solutions only for a limited number of simple charged boundary conditions. On the other hand, by solving it numerically or within some further approximations or limits, we can obtain the ionic profiles as well as the free energy of complex structures. For example, the free energy change of a charged globular protein approaching an oppositely charged lipid membrane. As any approximation, the PB theory has its limits of validity but in physiological conditions (electrolyte strength of about 0.1 M), it describes rather well the ionic distributions as long as the surfaces are not too highly charged. The PB theory produces good results for monovalent ions but misses some important features associated with multivalent counter-ions.

Throughout this chapter we present results for the following two limiting cases:

- The first is the *counter-ion only* case, where there is only one species of ions in solution neutralizing the charged surface: $n_-^0 = 0$ and $n_+^0 = n_0$. Then, the PB equation reads

$$\nabla^2 \phi = -\frac{4\pi e n_0 z_+}{\epsilon} e^{-e z_+ \phi / k_B T} \quad . \quad (6)$$

- The second is the *added electrolyte* (added salt) case where the system is placed in contact with an infinite reservoir of electrolyte. For simplicity, we treat only the symmetric monovalent electrolyte (e.g., $\text{Na}^+ \text{Cl}^-$): $z_{\pm} = \pm 1$ and $n_+^0 = n_-^0 = n_0$. Here

$$\nabla^2 \phi = \frac{8\pi e n_0}{\epsilon} \sinh \frac{e\phi}{k_B T} \quad . \quad (7)$$

We remark that it is rather straightforward to extend the above PB results to any multivalent ionic system, $z_- : z_+$.

The linearized PB equation: Debye-Hückel theory

In the case of low electrostatic potentials a very useful approximation can be used. In this case the PB equation (4) can be linearized (as long as $|\phi| < 25\text{mV}$) resulting in the famous Debye-Hückel (DH) theory.

$$\nabla^2 \phi \simeq \frac{8\pi e^2 n_0}{\epsilon k_B T} \phi(\mathbf{r}) = \lambda_D^{-2} \phi(\mathbf{r}) \quad , \quad (8)$$

The new parameter λ_D introduced above has units of length and is known as the *Debye-Hückel screening length*

$$\lambda_D = \sqrt{\frac{\epsilon k_B T}{8\pi e^2 n_0}} = (8\pi l_B n_0)^{-1/2} \sim n_0^{-1/2} \quad . \quad (9)$$

The screening length varies from about 3\AA in a strong ionic strength of 1 M of NaCl to about $1\mu\text{m}$ in pure water where the ionic strength of the dissociating OH^- and H^+ ions is 10^{-7} M. A useful formula to remember is that for n_0 measured in molar units, λ_D in Angstroms is given by

$$\lambda_D = \frac{3.05[\text{\AA}]}{\sqrt{n_0[\text{M}]} \quad . \quad (10)$$

The DH treatment gives a simple description to the many-body interactions between ions. It simply states that the interaction between any given pair of ions at distance $r = |\mathbf{r}|$ will decay exponentially due to the screening by all other cations and anions surrounding the ionic pair. Broadly speaking, this screened potential within the DH theory varies like $r^{-1} \exp(-r/\lambda_D)$. To a first approximation, one can say that for $r \leq \lambda_D$ the Coulombic interaction ($\sim r^{-1}$) is only slightly screened, while for $r > \lambda_D$ it is strongly (exponentially) screened.

In the remaining of this chapter we will consider the PB equation in various simple geometries. We will first discuss solutions of the PB equation in planar geometries and then mention with less details solutions in cylindrical and spherical geometries.

3 PB equation in planar geometry

3.1 A single charged surface

Counter-ion only

One of the simpler analytical solutions of the PB equation was formulated almost a century ago by Gouy (1910, 1917) and Chapman (1913). The problem they addressed is the profile of a cloud of counter-ions forming a diffusive *electric double-layer* close to a planar surface having a fixed surface charge density, σ . Without loss of generality, the surface charges are taken as anions ($\sigma < 0$) and the counter-ions as monovalent cations ($z_+ = 1$) having a density profile $n(z) = n_+(z)$. The system geometry is depicted on Fig. 1. The charged surface is at $z = 0$ and the counter-ions occupy the positive half plane, $z > 0$. As the $z = 0$ charged surface is infinite, the system is translationally invariant in the perpendicular x, y directions and the PB equation reduces to an ordinary differential equation

$$\phi''(z) = -\frac{4\pi en_0}{\epsilon} e^{-e\phi/k_B T} \quad , \quad (11)$$

with the boundary condition

$$\left. \frac{d\phi}{dz} \right|_{z=0} = -\frac{4\pi}{\epsilon} \sigma > 0 \quad . \quad (12)$$

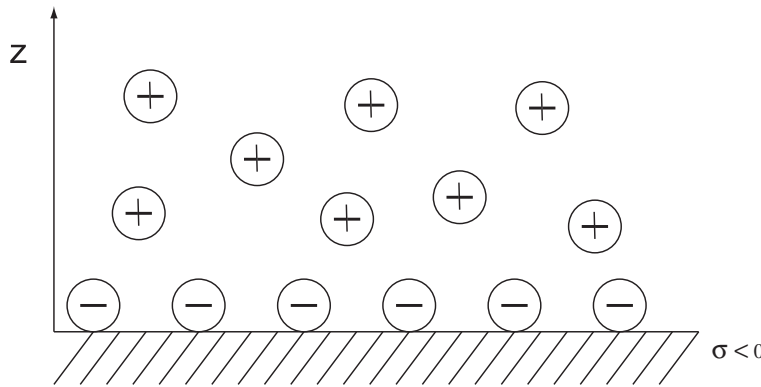


Figure 1. Schematic illustration of the electric double layer problem for the counter-ion only case. A negative surface with surface charge density σ is placed at $z = 0$, while its counter-ions are released in the solution. The surface is infinite in the (x, y) plane. Counter-ions are attracted to the surface and create a density profile, $n(z)$.

Equation (11) is a second-order differential equation. Using the boundary condition (12) it can be integrated analytically, yielding the following potential and ionic profile

$$\phi(z) = \frac{2k_B T}{e} \ln(z + b) + \phi_0 \quad , \quad (13)$$

$$n(z) = \frac{1}{2\pi l_B} \frac{1}{(z+b)^2} ,$$

where ϕ_0 is a reference potential and the length b is called the *Gouy-Chapman length*

$$b = \frac{\varepsilon k_B T}{2\pi e |\sigma|} = \frac{e}{2\pi |\sigma| l_B} \sim \sigma^{-1} . \quad (14)$$

Whereas the Bjerrum length is a measure of the electrostatic interactions in units of $k_B T$ and is constant of about 7\AA for aqueous solutions at room temperature, the Gouy-Chapman length is inversely proportional to σ , the surface charge density. For strongly charged surfaces, b is only a few Angstroms. Although the entire profile is diffusive as it decays algebraically, a simple meaning of b is that counter-ions accumulated in the layer of thickness b close to the surface have an integrated charge (per unit area) of $\frac{1}{2}|\sigma|$, balancing half of the surface charge. Note also that the potential has a logarithmic divergence as $z \rightarrow \infty$. This is associated with the infinite extent of the charged surface at $z = 0$. On the other hand, the electric field: $\mathbf{E} = -\nabla\phi$ decays to zero as it should for $z \rightarrow \infty$. On Fig. 2 we present the potential and ionic profile for a surface density of $\sigma = -e/250\text{\AA}$. The figure shows clearly the build-up of the diffusive layer of counter-ions attracted to the negatively charged surface, reaching a limiting value of $n_+(0) = 1.16\text{ M}$. The Gouy-Chapman length is here $b \simeq 5.71\text{\AA}$.

We discuss next the case where the charged surface is placed in contact with a electrolyte bath. Here the potential will decay to zero far away from the surface, even for charged surfaces of infinite extent, because of the screening by the bulk electrolyte reservoir.

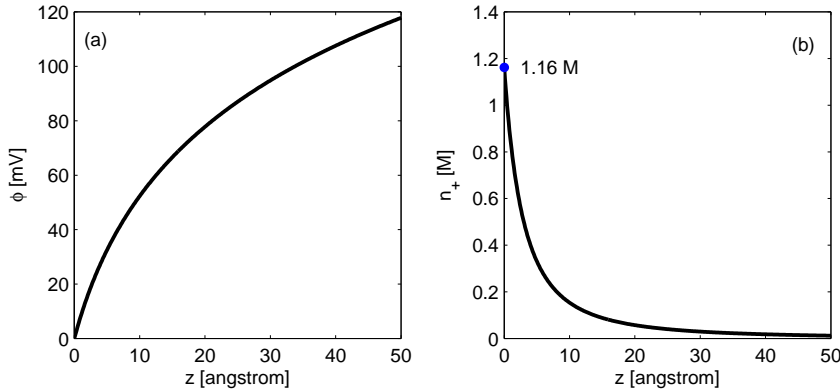


Figure 2. The electric double layer for a single charged surface in contact with an aqueous solution of monovalent cations. The charged surface is at $z = 0$ with $\sigma = -e/250\text{\AA}^2$. (a) Potential profile ϕ as function of the distance from the surface, z . The zero of the potential is taken at the surface. (b) Density profile of the counter-ions, n_+ as function of the distance z . The value at the surface is $n_+(0) = 1.16\text{ M}$ and the Gouy-Chapman length is $b \simeq 5.71\text{\AA}$.

Added electrolyte

We look now at another case of experimental interest where the charged surface at $z = 0$ is placed in contact with an electrolyte bath. On the surface, the same boundary condition (12) holds. For simplicity, we will consider a monovalent electrolyte $z_{\pm} = \pm 1$. In the bulk, far away from the surface ($z \rightarrow \infty$), we know that $n_{\pm}(\infty) = n_0$ where n_0 is the electrolyte bulk concentration.

The PB equation (7) can be integrated for this model system, yielding an analytical solution for the potential and ionic densities,

$$\begin{aligned}\phi(z) &= -\frac{2k_{\text{B}}T}{e} \ln \frac{1 + \gamma e^{-z/\lambda_{\text{D}}}}{1 - \gamma e^{-z/\lambda_{\text{D}}}} , \\ n_{\pm} &= n_0 \left(\frac{1 \pm \gamma e^{-z/\lambda_{\text{D}}}}{1 \mp \gamma e^{-z/\lambda_{\text{D}}}} \right)^2 ,\end{aligned}\quad (15)$$

where the parameter γ is the positive root of a quadratic equation,

$$\gamma = -\frac{b}{\lambda_{\text{D}}} + \sqrt{\left(\frac{b}{\lambda_{\text{D}}}\right)^2 + 1} ,\quad (16)$$

and the surface potential $\phi_{\text{s}} = \phi(0)$ is related to γ by eq. (15)

$$\phi_{\text{s}} = -\frac{4k_{\text{B}}T}{e} \operatorname{arctanh}(\gamma) .\quad (17)$$

Once the potential profile is known, the two ionic profiles can be simply calculated from the Boltzmann distribution: $n_{\pm}(z) = n_0 \exp(\mp e\phi(z)/k_{\text{B}}T)$ as is depicted on Fig. 3. The negatively charged surface attracts the counter-ions and repels the co-ions. The ratio b/λ_{D} is inversely proportional to the surface density. For small surface charge and/or high electrolyte strength, b/λ_{D} is large, yielding $\gamma \simeq \lambda_{\text{D}}/2b$, and

$$\phi(z) \simeq \phi_{\text{s}} e^{-z/\lambda_{\text{D}}} \simeq -\frac{2k_{\text{B}}T}{e} \frac{\lambda_{\text{D}}}{b} e^{-z/\lambda_{\text{D}}} ,\quad (18)$$

which coincides with the DH (linearized) limit of the PB equation (8). Note the difference between the counter-ion case where the potential diverges logarithmically, eq. (13), and the electrolyte-added case, eq. (15), where the potential decays to zero. In the limit of weak surface potential (or weak surface charge) the potential decays exponentially, eq. (18), with the Debye-Hückel screening length, λ_{D} , as its characteristic length. Within the PB treatment, eq. (15) is the exact solution for any amount of electrolyte and surface charges. It interpolates between these two limits.

The Grahame equation & the Contact theorem

The PB equation can be integrated once and leads to a relation, known as the *Grahame equation*, and also as the *Contact theorem*, Grahame (1947), Israelachvili (1992). This is a relation between the surface charge density σ and the limiting value of the ionic density

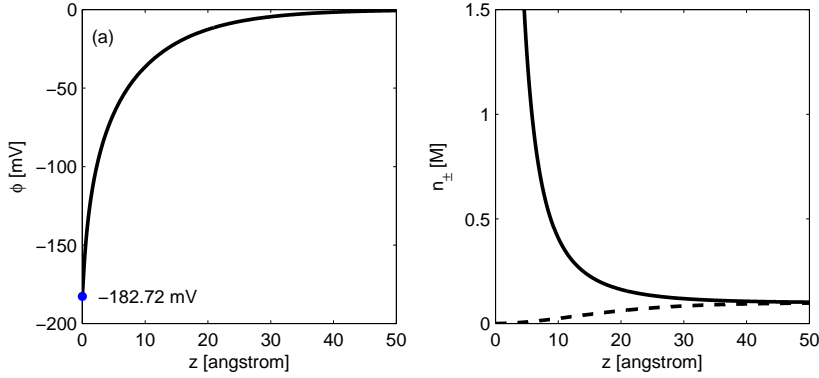


Figure 3. The electric double layer for a single charged surface in contact with a 1:1 monovalent electrolyte reservoir of concentration $n_0 = 0.1$ M. The charged surface is at $z = 0$ with $\sigma = -e/25 \text{ \AA}^2$. This σ is ten times larger than the value used in Fig. 2. (a) Potential profile ϕ as function of distance from the surface, z . The value of the surface potential is $\phi_s \simeq -182.7$ mV. (b) Density profile of the counter-ions, n_+ (solid line) and co-ions n_- (dashed line) are plotted as function of the distance z . The value at the surface is $n_+(0) \simeq 116.6$ M (for the co-ions profile to be visible, the diagram is cut at 1.5 M).

profile at the boundary, $n_{\pm}(z=0)$.

$$\sigma^2 = \frac{\varepsilon k_B T}{2\pi} [n_+(0) + n_-(0) - 2n_0] \simeq \frac{\varepsilon k_B T}{2\pi} [n_+(0) - 2n_0] \quad , \quad (19)$$

and

$$\sigma^2 = \frac{\varepsilon k_B T}{\pi} n_0 \left[\cosh \frac{e\phi_s}{k_B T} - 1 \right] \quad ,$$

For large ϕ_s , $n_+(0)/n_-(0) = \exp(2e|\phi_s|/k_B T) \gg 1$, and $n_-(0)$ is neglected in the above equation.

For example, for a surface charge density of one electronic charge per 25 \AA^2 (as in Fig. 3) and an ionic strength of $n_0 = 0.1$ M, the limiting value of the counter-ion density at the surface is $n_+(0) \simeq 116.6$ M.

3.2 Modified Poisson-Boltzmann equation

As we saw in the preceding section, the density of the accumulated counter-ions at the surface can reach very high, sometimes unrealistic values. A simple modification of the PB equation allows a remedy of this problem. In its modified form the only other added

ingredient is the entropy of the solvent in addition to that of the ions. This is especially of importance when the counter-ions have a large size and/or are multivalent.

In the case of a 1:1 electrolyte the PB equation with the solute entropy modification results in the following equations for the profile densities and potential, Borukhov *et al* (1997)

$$n_{\pm}(z) = \frac{n_0 e^{\mp e\phi/k_B T}}{1 - \varphi_0 + \varphi_0 \cosh(e\phi/k_B T)} \quad , \quad (20)$$

$$\nabla^2 \phi = -\frac{4\pi e}{\varepsilon} (n_+ - n_-) = \frac{8\pi e n_0}{\varepsilon} \frac{\sinh(e\phi/k_B T)}{1 - \varphi_0 + \varphi_0 \cosh(e\phi/k_B T)} \quad , \quad (21)$$

where $\varphi_0 = 2a^3 n_0$ is the volume fraction of the ions at bulk electrolyte concentration n_0 , and a is taken as the molecular size of both the solute and solvent. It is easy to see from eq. (20), that the counter-ions have a Fermi-Dirac like distribution. For small potentials, $e\phi/k_B T \ll 1$, the distribution reduces to the usual Boltzmann one, while for high potential, *e.g.*, close to a highly charged surface the counter-ion density saturates at close packing densities of $1/a^3$. This is very useful for multivalent counter-ions, where the regular PB theory gives unreasonable high values of ionic densities close to charged interfaces. As an example we show in Fig. 4 the modified and the regular PB profiles for a 1:1 electrolyte. Large ion size, $a = 8 \text{ \AA}$ is chosen to emphasize the saturation effect in the modified PB profile close to the charged surface. Note that the modified PB has a lower limiting value, $n_+(0)$, as well as a saturated accumulated layer of counter-ions close to the surface.

It is also easy to derive the modified Grahame equation relating the surface charge density σ with the counter-ion density at the surface. Neglecting the contribution of the co-ions at the surface, $n_-(0) \ll 1$, the Grahame equation, Borukhov *et al* (1997), reads

$$\sigma^2 \simeq \frac{\varepsilon k_B T}{2\pi} \frac{1}{a^3} \ln \frac{1 - 2a^3 n_0}{1 - a^3 n_+(0)} \quad . \quad (22)$$

Similarly, the surface charge density can be related with the surface potential ϕ_s by relating $n_+(0)$ to ϕ_s from eq. (20). Note that in the limit of small a , by expanding the logarithm in eq. (22), the Grahame equation (19) for the regular PB case is recovered.

3.3 Two planar surfaces

The PB equation can be solved for two planar surfaces. We will restrict ourselves to the case of two equally charged surfaces, located at $z = \pm d/2$, each having a charge density $\sigma < 0$ as is depicted on Fig. 5. Generalizations to non-equal surface charges exist as well, Parsegian and Gingell (1972). For planar and infinite surfaces, the PB equation reduces to an ordinary differential equation depending only on the coordinate z . We will consider separately the counter-ion only and added-electrolyte cases.

It is instructive to write down the electrostatic free energy for the two-surface problem. It comprises of the electrostatic energy and the entropy of the ions in solution (without considering the modifications of Sec. 3.2).

$$\mathcal{F} = U - TS = \int f d^3\mathbf{r} = \text{Area} \cdot \int f dz \quad ,$$

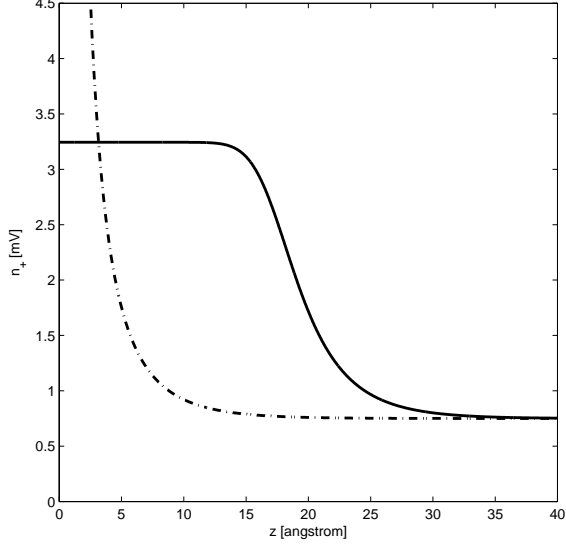


Figure 4. Comparison of the modified PB profile (MPB – solid line) having $a = 8 \text{ \AA}$, with the regular PB one (PB – dash-dotted line). The surface charge density is $\sigma = -e/25 \text{ \AA}^2$ and the 1:1 electrolyte ionic strength is $n_0 = 0.75 \text{ M}$. Note that while the PB value at the surface is $n_+(0) \simeq 117.7 \text{ M}$, the modified PB density saturates at $n_+(0) \simeq 3.24 \text{ M}$.

$$f = \frac{\varepsilon}{8\pi} (\nabla\phi)^2 + k_B T \left(n_+(r) \ln \frac{n_+(r)}{n_0} + n_-(r) \ln \frac{n_-(r)}{n_0} - [n_+(r) + n_-(r) - 2n_0] \right). \quad (23)$$

From the free energy per unit area \mathcal{F}/Area , we can calculate the osmotic pressure by taking a variation with respect to the inter-surface spacing d , while keeping the temperature and species chemical potentials fixed,

$$\Pi = - \frac{1}{\text{Area}} \left. \frac{\delta\mathcal{F}}{\delta d} \right|_{T,\mu}. \quad (24)$$

For the symmetric case of two equally charged surfaces, the profiles are symmetric about the mid-plane located at $z = 0$, yielding there a zero electric field, $E = 0$. By taking the full variation of the free energy, eq. (23), it can be shown that the pressure is simply equal to the excess of osmotic pressure calculated at the mid-plane with respect to the bulk electrolyte solution

$$\frac{\Pi}{k_B T} = \sum_i [n_i(z=0) - n_i^0]. \quad (25)$$

The osmotic pressure can be calculated at any point in the solution. Although the expression is different, its value agrees with the above expression calculated at the mid-plane.

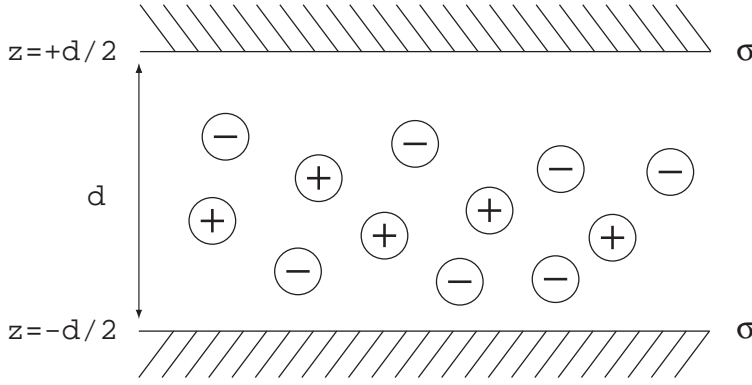


Figure 5. Schematic illustration of the two-surface system. The charged and planar surfaces are located at $z = \pm d/2$, and separated by a distance d . The surface charge is taken to be negative and is neutralized by the ions in solution. In the symmetric case, σ_1 and σ_2 are equal to the same value σ . For counter-ion only case, the two-surface charge is neutralized by the counter-ions. When electrolyte is added, the system is couple with an electrolyte reservoir of density $n_{\pm}^0 = n_0$.

3.3.1 Counter-ions only

For a symmetric two-plate system, it is enough to consider the interval $[0, d/2]$ because of the $z \leftrightarrow -z$ symmetry. The boundary conditions are $d\phi/dz|_{z=d/2} = (4\pi/\varepsilon)\sigma$ and $d\phi/dz|_{z=0} = 0$. Let us call $n(z) = n_+(z)$ and denote by n_m and ϕ_m the values of the density and potential at the mid-plane, respectively. For these boundary conditions, the PB equation can now be solved analytically.

$$\begin{aligned}\phi(z) &= \frac{k_B T}{e} \ln(\cos^2 Kz) < 0 \quad , \\ n(z) &= n_m e^{-e\phi(z)/k_B T} = \frac{n_m}{\cos^2 Kz} \quad ,\end{aligned}\tag{26}$$

where the new length in the problem $1/K$ is related to n_m by

$$K^2 = \frac{2\pi e^2}{\varepsilon k_B T} n_m \quad .\tag{27}$$

Using the boundary condition at $z = d/2$ we get a transcendental relation for K

$$Kd \tan(Kd/2) = -\frac{2\pi e\sigma}{\varepsilon k_B T} d = \frac{d}{b} \quad ,\tag{28}$$

where b is the Gouy-Chapman length defined in eq. (14). A typical counter-ion profile is shown in Fig. 6a for $\sigma = -e/750 \text{ \AA}^2$ and $d = 40 \text{ \AA}$.

The osmotic pressure [eq. (25)] calculated in the counter-ion only case is

$$\frac{\Pi(d)}{k_B T} = \frac{\varepsilon k_B T}{2\pi e^2} K^2 = \frac{1}{2\pi l_B} K^2 \quad .\tag{29}$$

Because K depends on other system parameters we discuss now separately two limits, depending on how strong the surface charge is.

Weak surface charges

For $d/b \ll 1$, the surface charge is weak. From eq. (27), $(Kd)^2 \simeq 2d/b \ll 1$. The pressure then is

$$\frac{\Pi(d)}{k_{\text{B}}T} \simeq -\frac{1}{d} \frac{2\sigma}{e} = \frac{1}{\pi l_{\text{B}}} \frac{1}{d} . \quad (30)$$

This regime is called the *ideal gas* regime as is apparent from the above pressure expression. The density (per unit volume) of the counter-ions is almost constant between the two plates and is equal to $2|\sigma|/(ed)$. The main contribution to the pressure comes from the ideal-gas like pressure of the cloud of counter-ions. Note that this regime occurs only for small separations, $d < b$. For weakly charged surfaces, b is relatively large and this regime can be seen for separations in the range of a few Angstroms or more.

Strong surface charges

Here, from eq. (27), $d/b \gg 1$ and $Kd \rightarrow \pi$. The leading order term in the pressure is then

$$\frac{\Pi(d)}{k_{\text{B}}T} \simeq \frac{\pi}{2l_{\text{B}}} \frac{1}{d^2} = \frac{\pi \varepsilon k_{\text{B}}T}{2e^2} \frac{1}{d^2} . \quad (31)$$

It is interesting to note that the above pressure equation is independent of the surface charge density and is closely related to the *Langmuir equation*, as is discussed in Israelachvili (1992). But one should recall that this equation holds for counter-ions only. As soon as one adds electrolyte, the pressure expression changes as is shown in the next section.

3.3.2 Added electrolyte

The PB equation is now considered for an electrolyte solution between two charged surfaces, restricting ourselves to a 1:1 symmetric and monovalent electrolyte, eq. (7). However, here the exact solution can only be expressed in terms of an elliptic integral. Let us define a dimensionless potential $\eta \equiv -e\phi/k_{\text{B}}T$ so that $\eta > 0$ for $\sigma < 0$. At the mid-plane $\eta_{\text{m}} \equiv \eta(z=0)$ and on the charged surface $\eta_{\text{s}} \equiv \eta(d/2)$. The PB equation and boundary conditions are now written in terms of η

$$\frac{d^2\eta}{dz^2} = \lambda_{\text{D}}^{-2} \sinh \eta , \quad (32)$$

$$\left. \frac{d\eta}{dz} \right|_{z=d/2} = \frac{2}{b} \quad \text{and} \quad \left. \frac{d\eta}{dz} \right|_{z=0} = 0 . \quad (33)$$

First integration from the mid-plane position ($z=0$) to an arbitrary z gives

$$\lambda_{\text{D}} \frac{d\eta}{dz} = \sqrt{2 \cosh \eta(z) - 2 \cosh \eta_{\text{m}}} . \quad (34)$$

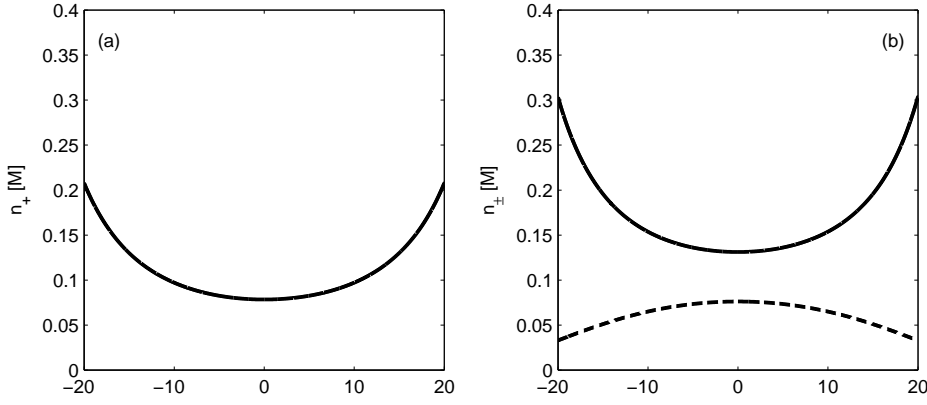


Figure 6. Ion density profiles between two identical charged surfaces with $\sigma = -e/750 \text{ \AA}^2$ each, at separation $d = 40 \text{ \AA}$ located at $z = \pm 20 \text{ \AA}$. In (a) the $n_+(z)$ profile is plotted from eqs. (26)-(28) for the counter-ion only case, while in (b) n_+ and n_- (solid and dashed lines, respectively) are plotted for 1:1 electrolyte with $n_0 = 0.1 \text{ M}$. See eqs. (35)-(37). As $b \simeq 17.2 \text{ \AA}$, and $\lambda_D \simeq 9.75 \text{ \AA}$, we are in between the Intermediate and DH regions of Fig. 7 where $d > b > \lambda_D$.

A further definite integration gives an elliptic integral

$$\frac{z}{\lambda_D} = \int_{\eta_m}^{\eta} \frac{d\eta'}{\sqrt{2 \cosh \eta' - 2 \cosh \eta_m}} \quad . \quad (35)$$

The boundary condition (33) can be inserted in eq. (34) yielding

$$\cosh \eta_s = \cosh \eta_m + \frac{2\lambda_D^2}{b^2} \quad , \quad (36)$$

while the second boundary condition at $z = d/2$ is expressed as

$$\frac{d}{2\lambda_D} = \int_{\eta_m}^{\eta_s} \frac{d\eta}{\sqrt{2 \cosh \eta - 2 \cosh \eta_m}} \quad . \quad (37)$$

The last three equations (35)-(37) completely determine the potential $\eta(z)$ and the two species density profiles, $n_{\pm}(z) = n_0 \exp(\pm\eta(z))$ and their mid-plane values $n_m^{\pm} = n_0 \exp(\pm\eta_m)$, as function of the three system parameters: the inter-surface spacing d , the surface charge density σ (or equivalently b), and the electrolyte bulk ionic strength n_0 (or equivalently λ_D). An example of the counter-ion and co-ion profiles is shown in Fig. 6b. Note that in the figure, the three lengths are chosen such that $d > b > \lambda_D$, placing us in between the DH and Intermediate regions of Fig. 7.

Once the profiles are calculated, the pressure has a simple dependence on the mid-plane properties.

$$\frac{\Pi(d)}{k_B T} = n_m^+ + n_m^- - 2n_0 = 2n_0 (\cosh \eta_m - 1) \quad . \quad (38)$$

We end the treatment of the 1:1 electrolyte solution between two identically charged surfaces by giving several limiting expressions for the pressure. The exact form can be obtained from the numerical solution of eqs. (35)-(37) as outlined above. Figure 7 summarizes the four different regimes in the $(\lambda_D/d, b/d)$ plane. More details about these limiting expressions can be found in Andelman (1995).

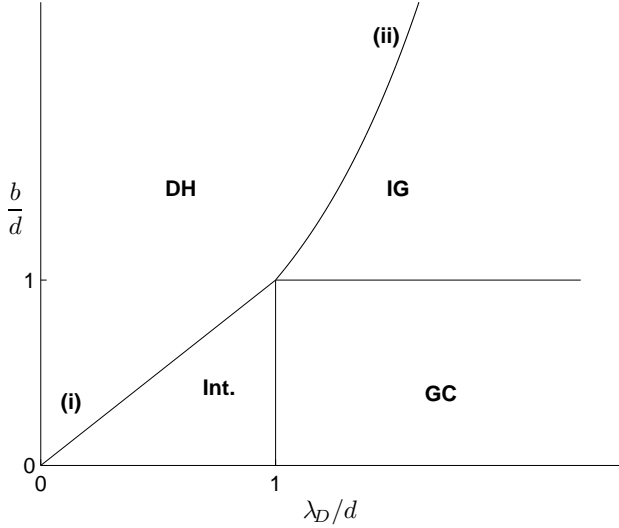


Figure 7. Schematic representation of the various limits of the PB equation for two flat and equally charged surfaces at separation d . The diagram is plotted in terms of two dimensionless ratios: b/d and λ_D/d , where b , d and λ_D are the Gouy-Chapman length, the inter-surface spacing and the Debye-Hückel length, respectively. The four regions discussed in the text are: the Ideal-Gas (IG), the Gouy-Chapman (GC), Intermediate (Int.) and the Debye-Hückel (DH) regions. They are separated by 3 straight lines: $b = \lambda_D$, $b/d = 1$, $\lambda_D/d = 1$ and a parabolic one $b/d = (\lambda_D/d)^2$. The DH region is further divided into two sub-regimes: (i) large d and (ii) small d spacing.

Ideal-gas region

In the limit of $b/d \gg 1$ and $(\lambda_D/d)^2 \gg b/d$, the pressure reduces to the expression obtained for the counter-ion only case in the limit of small surface charge, eq. (30). The validity of this *Ideal-gas* region is for low electrolyte ionic strength and small surface charge.

$$\frac{\Pi(d)}{k_B T} \simeq -\frac{1}{d} \frac{2\sigma}{e} = \frac{1}{\pi l_B b} \frac{1}{d} . \quad (39)$$

Gouy-Chapman region

In the region defined by $\lambda_D/d \gg 1$ and $b/d \ll 1$ where the electrolyte strength is still weak, but for large surface charge density, the expression for the pressure coincides with

the other limit, eq. (31). This region is called the *Gouy-Chapman* region

$$\frac{\Pi(d)}{k_B T} \simeq \frac{\pi \varepsilon k_B T}{2e^2} \frac{1}{d^2} = \frac{\pi}{2l_B} \frac{1}{d^2} . \quad (40)$$

Intermediate region

Within the limits of validity $\lambda_D/d \ll 1$ and $b \ll \lambda_D$, in the *Intermediate* region, the surface potential is rather large $\eta_s \geq 1$ and $\gamma = \tanh(\eta_s/4) \approx 1$. The PB equation cannot be linearized. On the other hand, the mid-plane potential is small $\eta_m = 8\gamma \exp(-d/2\lambda_D) \ll 1$, and the coupling between the two surfaces is weak.

$$\frac{\Pi(d)}{k_B T} = n_0 \eta_m^2 \simeq \frac{8}{\pi l_B \lambda_D^2} e^{-d/\lambda_D} . \quad (41)$$

Debye-Hückel region

The last region is the DH region where the PB equation can be linearized. This region can further be divided into two limits. For large d denoted as case (i) in Fig. 7, $\lambda_D/d \ll 1$ and $b \gg \lambda_D$, and for small d denoted as case (ii) in Fig. 7, $\lambda_D/d \gg 1$ and $(\lambda_D/d)^2 \ll b/d$.

The pressure of the linearized DH equation in both limits is given by

$$\frac{\Pi(d)}{k_B T} \simeq \frac{1}{2\pi l_B b^2} \frac{1}{\sinh^2(d/2\lambda_D)} , \quad (42)$$

which reduces in the large d separation, $d \gg \lambda_D$, case (i), to the well-known result

$$\frac{\Pi(d)}{k_B T} \simeq \frac{2}{\pi l_B b^2} e^{-d/\lambda_D} , \quad (43)$$

and for small d , $d \ll \lambda_D$, case (ii), to

$$\frac{\Pi(d)}{k_B T} \simeq \frac{2}{\pi l_B} \frac{\lambda_D^2}{b^2 d^2} . \quad (44)$$

4 Poisson-Boltzmann equation in cylindrical coordinates

The PB equation can be solved in cylindrical geometry to model the accumulation of charges around rod-like and charged objects such as rigid polyelectrolytes or elongated colloidal particles. In several situations analytical solutions exist, while in others one needs to rely on numerical solutions and approximations.

In the case where we have a solution of rod-like molecules (or cylindrical colloidal particle) we can construct a *cell model*. The model is composed of two concentric cylinders with an ionic solution in between them (neglecting any finite size of the cylinder caps). See Fig. 8. The inner cylinder models a charged and elongated particle, while the outer cylinder defines the boundary of the specific volume per charged (cylindrical) particle in case of a multi-particle solution. Because of the cylindrical symmetry it is clear

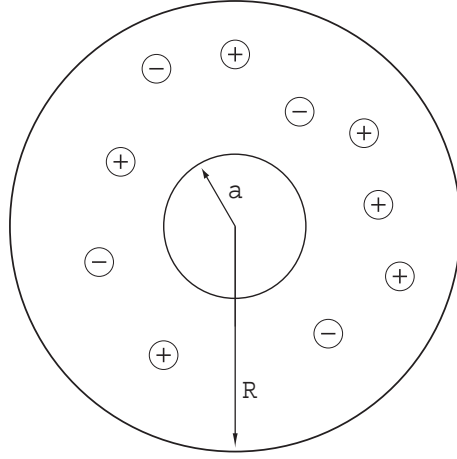


Figure 8. Schematic illustration of the two-cylinder problem. The aqueous solution is bounded between two concentric cylinders. The inner one at $r = a$ is negatively charged, $\sigma < 0$. On the outer cylinder, $r = R$, the electric field vanishes as the entire cell is electrically neutral.

that the potential $\phi(r, \theta, \varphi)$ depends only on the coordinate r , measured from the major axis of the cylinder at the origin. The inner cylinder of radius a has a surface charge density (per unit area) $\sigma < 0$. Alternatively, we can define on the inner cylinder the charge line density ρ (number of charges per unit length)

$$\rho \equiv 2\pi a |\sigma| e \quad . \quad (45)$$

The outer cylinder of radius R defines the total volume of the aqueous solution per charged object (cylinder). From the cylindrical symmetry and the requirement to have charge neutrality within the cell of radius R , the electric field has to vanish at $r = R$. The boundary conditions then are

$$\left. \frac{d\phi}{dr} \right|_{r=a} = -\frac{4\pi}{\epsilon} \sigma = \frac{2e \rho}{\epsilon a} \quad , \quad (46)$$

$$\left. \frac{d\phi}{dr} \right|_{r=R} = 0$$

4.1 The linearized PB equation: Debye-Hückel theory

We discuss the PB equation in the linear DH limit. As in Sec. 2, the linear DH gives:

$$\nabla^2 \phi = \frac{d^2 \phi}{dr^2} + \frac{1}{r} \frac{d\phi}{dr} = \lambda_D^{-2} \phi(r) \quad , \quad (47)$$

This equation is the modified Helmholtz equation in cylindrical coordinates and has an analytical solution satisfying the boundary conditions (46):

$$\frac{e\phi}{k_B T} = -\frac{2}{b\kappa_D} \frac{K_0(\kappa_D r) I_1(\kappa_D R) + I_0(\kappa_D r) K_1(\kappa_D R)}{K_1(\kappa_D a) I_1(\kappa_D R) - I_1(\kappa_D a) K_1(\kappa_D R)} \quad , \quad (48)$$

where $\kappa_D \equiv \lambda_D^{-1}$ is the inverse of the Debye-Hückel screening length, b the Gouy-Chapman length as in eqs. (9) and (11), and the functions I_n and K_n are the n^{th} order modified Bessel functions of the first and second kind, respectively.

The limit when the outer cylinder radius goes to infinity, $R \rightarrow \infty$, corresponds to the infinite dilution limit of one charged object (cylinder) embedded in an aqueous ionic solution. Then eq. (48) reduces to

$$\frac{e\phi}{k_B T} = -\frac{2}{b\kappa_D} \frac{K_0(\kappa_D r)}{K_1(\kappa_D a)} . \quad (49)$$

The above expression decays exponentially to zero for $\kappa_D r \gg 1$

$$\phi \sim \frac{1}{\sqrt{r}} e^{-\kappa_D r} . \quad (50)$$

4.2 The non-linear PB solution: counter-ion only and Manning condensation

The non-linear PB equation in cylindrical geometry has an analytical solution for the counter-ion only case, Fuoss *et al* (1951). We note that rather recently a additional analytical solution has been derived for the added-electrolyte case in a certain limit, Tracy and Widom (1997). This is the limit of infinite dilution ($R \rightarrow \infty$) and vanishing inner cylinder radius, $\kappa_D a \rightarrow 0$. However, we will restrict ourselves to the counter-ion only case and discuss the interesting phenomena of counter-ion condensation in the infinite dilution limit, known as the Manning condensation, Manning (1969), Oosawa (1971), Le Bret and Zimm (1984). This condensation phenomenon cannot be obtained within the linearized DH regime.

Let us consider again the PB equation for two concentric cylinders, but this time with counter-ions only. The PB equation and the boundary conditions at $r = a$ and $r = R$ is written for the dimensionless potential $\eta = -e\phi/k_B T$

$$\frac{d^2\eta}{dr^2} + \frac{1}{r} \frac{d\eta}{dr} = 4\pi l_B n_0 e^\eta , \quad (51)$$

and

$$\left. \frac{d\eta}{dr} \right|_{r=a} = 4\pi l_B \frac{\sigma}{e} = -\frac{2l_B \rho}{a} \quad \text{and} \quad \left. \frac{d\eta}{dr} \right|_{r=R} = 0 . \quad (52)$$

It is possible to map exactly the two-cylinder problem into the simpler two-plate problem discussed earlier in Sec. 3.3.1, Burak (2004b). This mapping is an alternative way of looking at the original two-cylinder solution derived by Fuoss *et al* (1951) and detailed in Oosawa (1971).

First we change the distance variable r into u

$$u = \ln \frac{r}{a} , \quad (53)$$

yielding the PB equation

$$\frac{d^2\eta}{du^2} = 4\pi \tilde{n}_0 e^{\eta+2u} , \quad (54)$$

with a renormalized charge density \tilde{n}_0 defined as

$$\tilde{n}_0 = l_B a^2 n_0 \quad . \quad (55)$$

Making another change of variables for the potential

$$\psi = -\eta - 2u \quad , \quad (56)$$

we obtain an exact mapping of the original cylindrical problem into an equivalent PB for two planar surfaces:

$$\frac{d^2\psi}{du^2} = -4\pi\tilde{n}_0 e^{-\psi} = -4\pi\tilde{n}(\psi) \quad , \quad (57)$$

with two boundary conditions

$$\left. \frac{d\psi}{du} \right|_{u=0} = 2(l_B\rho - 1) \quad \text{and} \quad \left. \frac{d\psi}{du} \right|_{u=d} = -2 \quad . \quad (58)$$

The mapping is done between the PB equation solved in cylindrical geometry for two concentric cylinders, and the PB equation solved in planar geometry for the counter-ions only case having two planar but *non-identical* charged surfaces. One surface at $u = 0$ has a surface charge density of $(1 - l_B\rho)/2\pi l_B$. This charge can be positive or negative. The second surface at $d = \ln(R/a)$ has a negative surface charge density of $-1/(2\pi l_B)$. The mapping between the two-cylinder problem and the two-plane problem is summarized in the Table below.

Before we detail the solution of the two concentric cylinder, let us introduce the concept of the *Manning condensation*. It can be easily understood from this mapping by thinking of the analog planar case in the large d separation. For $l_B\rho < 1$, the surface at $u = 0$ has the same sign as the counter-ions, while the surface at $u = d$ is attractive. When $d \rightarrow \infty$ the counter-ions will be repelled from the $u = 0$ surface and will "run away" to infinity, gaining both entropy and electrostatic attraction with the other surface. However, for $l_B\rho > 1$ the $u = 0$ surface is attractive for the counter-ions. When the other surface is taken to infinity, $d \rightarrow \infty$, some of the counter-ions will stay behind balancing entropy and electrostatic attraction, in such a way that the effective charge is always $\rho^* = 1/l_B$. This is the Manning condensation. It states that in infinite dilution (one charged cylinder) and without added salt, the effective charge density of the polyelectrolyte chain never exceeds $1e$ per $l_B \simeq 7 \text{ \AA}$.

We now mention the solution for the two concentric cylinders representing a finite concentration of charge rod-like molecules in the solution. Returning to the mapping introduced above, the charges on the two planar surfaces are not identical. The parameter $1 - l_B\rho$ is the charge density on the surface at $u = 0$, and it can be positive ($l_B\rho < 1$) or negative ($l_B\rho > 1$). The non-linear case of no-added electrolyte for two concentric cylinders was solve by Fuoss *et al* (1951). Here we use the mapping to the planar geometry to get the same results within a different method. The charge density profile expressed in the cylindrical geometry is

$$n(r) = \frac{1}{2\pi l_B r^2} \times \begin{cases} B^2 [\sinh(B \ln \frac{r}{R} - \operatorname{arctanh} B)]^{-2} & \rho < \rho^* \\ (\ln(r/R) + 1)^{-2} & \rho = \rho^* \\ B^2 [\sin(B \ln \frac{r}{R} - \operatorname{arctan} B)]^{-2} & \rho > \rho^* \end{cases} \quad , \quad (59)$$

	distance	potential	ref. density	inner b.c.	outer b.c.
cylinder	r $a \leq r \leq R$	$\eta = -\frac{e\phi}{k_B T}$	n_0	$\frac{2l_B \rho}{a}$	0
planar	$u = \ln \frac{r}{a}$ $0 \leq u \leq d = \ln \frac{R}{a}$	$\psi = -\eta - 2u$	$\tilde{n}_0 = l_B a^2 n_0$	$\frac{1-l_B \rho}{2\pi l_B}$	$-\frac{1}{2\pi l_B}$

Table 1. Mapping between PB equation in cylindrical and planar geometries

where the critical value ρ^* is given by

$$\rho^* = \frac{1}{l_B} \frac{\ln(R/a)}{\ln(R/a) + 1}, \quad (60)$$

and has the limit of $\rho^* \rightarrow 1/l_B$ for infinite dilution, $R/a \rightarrow \infty$, in agreement with the Manning condensation threshold. The only other parameter in eq. (59) is the integration constant B , which can be obtained from the boundary condition at the inner cylinder $r = a$. Depending on the value of ρ with respect to ρ^* , B can be obtained by inverting the following equation

$$\rho = \frac{1}{l_B} \times \begin{cases} 1 - B \coth[B \ln(R/a) + \operatorname{arctanh} B] & \rho < \rho^* \\ 1 - B \cot[B \ln(R/a) + \operatorname{arctan} B] & \rho > \rho^* \end{cases}, \quad (61)$$

5 Poisson-Boltzmann equation in spherical coordinates: charged colloids

Dispersion of small (submicron) particles in a liquid solution is called a colloidal suspension. The suspension can be stabilized against van der Waals attractive forces by several means. In aqueous solutions if the particles are charged, the competition between the electrostatic repulsion and the van der Waals attraction can stabilize the suspension. This is the idea behind the famous DLVO theory of Deryagin, Landau, Verwey and Overbeek, Deryagin and Landau (1941), Verwey and Overbeek (1948), where the attractive van der Waals attraction is balanced with screened repulsive electrostatic repulsion, resulting in a secondary minimum for particle-particle interaction.

Let us now consider the limit of infinite particle dilution: one spherical charged particle immersed in a solution containing its counter-ions and possibly added salt. The PB equation can be solved in spherical coordinates. For a perfect spherical particle of radius a and charge Qe , the charge density is $\sigma = Qe/4\pi a^2$.

The linearized PB equation (the DH limit) in spherical coordinates is simply written

as:

$$\nabla^2 \phi = \frac{d^2 \phi}{dr^2} + \frac{2}{r} \frac{d\phi}{dr} = \lambda_D^{-2} \phi(r) \quad , \quad (62)$$

The linearization can be justified in presence of high added salt and moderate particle charge density. For one sphere problem, we require the potential and the electric field to vanish at infinity, while on the spherical surface, $r = a$, the potential boundary condition is

$$\begin{aligned} \left. \frac{d\phi}{dr} \right|_{r=a} &= -\frac{Qe}{\varepsilon a^2} \quad , \\ \left. \frac{d\phi}{dr} \right|_{r=\infty} &= 0 \end{aligned} \quad (63)$$

Clearly the solution of the linearized PB equation has the DH form in spherical coordinates: $\exp(-\kappa_D r)/r$, where $\kappa_D = 1/\lambda_D$. Together with the boundary condition we get

$$\frac{e\phi(r)}{k_B T} = \frac{Q l_B}{1 + \kappa_D a} \frac{e^{-\kappa_D (r-a)}}{r} \quad (64)$$

The linearized PB equation is correct only in the high salt limit, $\kappa_D a \gg 1$. However, even in lower salt concentration, it is useful to consider an *effective* particle charge Q_{eff} . Far away from the charged sphere, the non-linear PB solution will have an asymptotic solution behaving just like the linear PB solution, eq. (64), but with an effective charge Q_{eff} replacing the nominal charge Q of the sphere.

We concentrate on the case of a charged enough sphere such that $a/b = l_B Q/2a \gg 1$, where b is the same Gouy-Chapman length introduced in the planar geometry, eq. (11), and is equal here to $b = 2a^2/l_B Q$. In the very high salt limit, Q_{eff} is about equal to Q . As we lower the amount of salt, the correction to Q_{eff} is found to be

$$Q_{\text{eff}} = Q \left(1 - \frac{1}{4\kappa_D^2 b^2} + \dots \right) \quad (65)$$

At intermediate salt concentration, $\kappa_D a \simeq 1$, the behavior is non-monotonic (and will not be detailed here), while for $\kappa_D a \ll 1$ [but not smaller than $\exp(-l_B/2a)$], Q_{eff} saturates at a value, Ramanathan (1986, 1988) that does not depend on Q itself:

$$Q_{\text{eff}} = \frac{2a}{l_B} \ln \left[\frac{4}{\kappa_D a} \ln \left(\frac{1}{\kappa_D a} \right) \right] \quad (66)$$

Taking values of typical colloidal suspensions we have $a \simeq 200 \text{ \AA}$ and $Q=2000$. This gives us $a/b \simeq 35 \gg 1$. For high salt, Q_{eff} is slightly lower than 2000. As $\kappa_D a$ is lowered, Q_{eff} becomes much lower than Q and then reaches an effective value of about 400 for $\kappa_D a = 10^{-2}$. Namely, about a fifth of its original value. An interesting remark is that for a large range of low salinity, Q_{eff} is a weak function of Q , and depends mainly of the salt concentration and particle size a . Namely, different values of Q will roughly give the same Q_{eff} for the same salinity and particle size.

A similar notion of charge renormalization (Q_{eff}) was introduced by Alexander *et al* (1984), for a solution containing a finite concentration of particles. In the *absence*

of salt (counter-ion only), it was proposed that the potential far away from the charged spherical particles looks like a DH potential with an effective charge which is due to the presence of all other charged spheres, Belloni (1998). Roughly speaking Q_{eff} is equal to a/l_B multiplied by a logarithmic correction that depends on system parameters. However, this logarithmic correction is small and we remark the resemblance of this charge renormalization to that of eq. (66) above.

6 Beyond the PB treatment

In this chapter we concentrated on the relatively simple Poisson-Boltzmann equation and have shown how its solutions in different geometries: planar, cylindrical, spherical are related to several interesting physical problems. The PB theory is a mean-field one and as such it neglects fluctuations and correlations. In addition, it neglects the finite size of the ions and the fact that the solvent is not a continuous media. (But see Burak and Andelman (2000, 2001) and references therein for discrete solvent corrections.) At present, a unified theory that takes into account all corrections to PB is not available, but there are a number of attempts where specific corrections to PB have been proposed and studied in detail. We briefly mention some of these corrections (see also the chapter by Podgornik).

Strong deviations from PB behavior is seen in the cases where the concentration of ions in solution is very large. There, electrostatic interactions are highly screened and the specificity of ions, the structure of the water shell around them (hydration shell) and the ionic finite size and polarizabilities come into play. Molecular dynamic (MD) simulations have shown that the water shell around ions causes short-range attraction Guàrdia *et al* (1991). Another interesting effect for high electrolyte concentration, $n_0 > (2/\pi)l_B^{-3}$ electrolytes, are phase transitions and related critical phenomena as reviewed by Fisher (1994) and Levin (2002).

Several attempts have been made in the past to use liquid-state theories, Hansen and McDonald (1986), Rosenfeld and Ashcroft (1979), Henserson (1992), to improve upon the PB treatment by calculating the corrections due to correlations. Although these methods involved uncontrolled approximations (unlike perturbative methods), they are quite successful in high salt concentrations. We mention here only one variant called the *Anisotropic Hypernetted Chain* (AHNC) method. The ANHC involved integral equations and can be used in anisotropic charged systems such as ionic profiles close to charged surfaces, Henderson (1992), Kjellander (1996), Kjellander and Marčelja (1984) and (1985). For divalent counter-ions (such as Ca^{++}), ANHC calculations, in agreement with Monte-Carlo simulations and experiments, have confirmed attractive interaction between two highly-charged surfaces with inter-surface separation of a few Angstroms. This result has important consequences in the study of clays and zeolites. This attraction clearly goes beyond the PB treatment because it can be shown rigorously that equally charged surfaces always repel each other within the PB formalism, Neu (1999), Sader and Chan (1999) and (2000). Another correlation-induced attraction can be found from Monte-Carlo simulations, Moreira and Netz (2002), Guldbrand *et al* (1984), Kjellander *et al* (1992), Gronbech-Jensen *et al* (1997), Deserno *et al* (2003); and other analytical techniques: Attard *et al* (1984), Podgornik (1990), Pincus and Safran (1998), Netz and

Orland (2000), Burak and Andelman (2001). Corrections to PB can be quite substantial when the counter-ions in solution are multivalent and the surface charges are large.

The phenomenon of DNA condensation and aggregation in presence of multivalent counter-ions is another example where PB fails to provide the full physical picture. More details are given in the chapter of Podgornik. The attraction that causes the aggregation and condensation is especially strong in presence of trivalent and tetravalent counter-ions such as spermidine and spermine, Anderson and Record (1980), Raspaud *et al* (1998) and is a topic of numerous investigations, Bloomfield (1991), Rau and Parsegian (1992a, 1992b), Ha and Liu (1997), Gelbart *et al* (2000), Grosberg *et al* (2002), Burak *et al* (2003, 2004c)

7 Concluding remarks

In this chapter we reviewed some of the underlying principles behind the behavior of charges in solution. In particular, we considered the way ions in solution will react to the presence of charged boundary conditions, like a charged surface or particle. Considerable insight can be gained from simple models of one charged surface immersed in an ionic solution, or the forces that exist between two such surfaces as mediated by the ionic solution. Other geometries are also useful to consider. Charged cylinders can be thought of as models of long, rod-like and charged molecules, while spheres model colloidal particles.

The chapter mainly describes results obtained within the Poisson-Boltzmann formalism that is a mean-field approximation. Corrections to this theory are due to correlations and fluctuations of charge densities, and may play a substantial role.

The simple geometries of a plane, cylinder and sphere may be too simplified in some applications. The geometrical shape of charged membranes and macromolecules is often more complex. In addition, the shape often is not rigid but can deform at room temperature. Hence, the flexibility of the objects and its charge contributions has to be considered.

We close this chapter by mentioning two such examples. Biological membranes are two-dimensional flexible objects. A stack of membranes forming a lamellar system is shown on Fig. 9. When the membranes are charged, the most straightforward effect is a stiffening of the elastic constants. The exact expression of the bending modulus depends on the amount of salt and membrane thickness and charge. A simple result can be obtained in the linearized DH limit where the elastic bending modulus is increased by an amount proportional to

$$\frac{\sigma^2 \lambda_D^3}{\epsilon} \sim \frac{\lambda_D^3}{l_B b^2} . \quad (67)$$

When the charged membranes are composed of mixtures of charged and neutral lipids, the charges can rearrange themselves laterally on the membrane. This can lead to lateral phase separation and nucleation of charged domains.

Another example is related to the flexibility of charged polymers, depicted on Fig. 10. Polymers have a persistence length ℓ_p above which long chains behave as a random walk, while for lengths smaller than ℓ_p , the chain is nearly rigid, rod-like. As the chains become

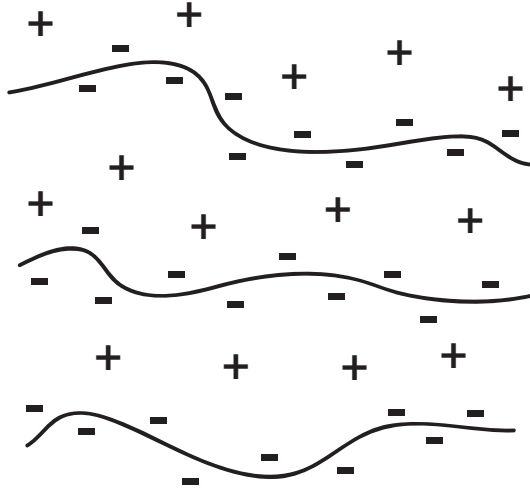


Figure 9. A schematic illustration of a lamellar stack of membranes. Each membrane is made of a charged bilayer. The entire stack is neutral. The membrane undulations depends on $k_B T$ and the elastic bending modulus.

charged, the main effect is the rigidifying of the chains resulting in an increase in the persistence length. Using the linearized PB equation, the electrostatic persistence length was calculated by Odijk (1977) and independently by Skolnick and Fixman (1977)

$$\ell_p = \frac{l_B \rho^2}{4\kappa_D^2} \quad (68)$$

where ρ is the line charge density (number of charges per unit length) on the chain. For highly charged chains such as DNA, and, in particular, in presence of multivalent counterions, this result has corrections which lead to possible chain instabilities and collapse. Such a phenomena has been observed for DNA as well as for synthetic polyelectrolytes.

Acknowledgements

I am indebted to Y. Burak for comments and to E. Mar-Or for technical assistance. The discussion of the PB solution in cylindrical geometry is based on the PhD thesis of Y. Burak (Tel Aviv University, 2004). This chapter was completed during a stay at the Isaac Newton Institute, University of Cambridge. I thank the Institute for its hospitality. Support from the U.S.-Israel Binational Science Foundation (B.S.F.) under grant No. 287/02 and the Israel Science Foundation under grant No. 210/01 is gratefully acknowledged.

References

Alexander S, Chaikin P M, Grant P, Morales J, and Pincus P, 1984, *J Chem Phys* **80** 5776.

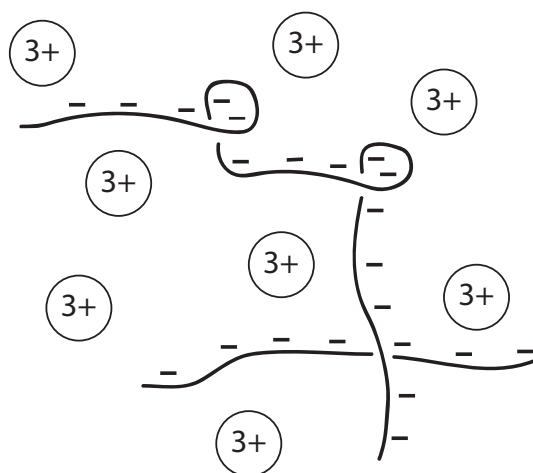


Figure 10. A schematic representation of a polyelectrolyte solution. The chains are negatively charged and the counter-ions are trivalent.

Andelman D, 1995, *Electrostatic Properties of Membranes: The Poisson-Boltzmann Theory*, chapter 12 in *Handbook of Biological Physics*, Volume 1, edited by Lipowsky R and Sackmann E, (Elsevier Science, Amsterdam)

Anderson C F and Record Jr M T, 1980, *Biophys Chem* **11** (1980) 353.

Attard P, Mitchell D J, and Ninham B W, 1988, *J Chem Phys* **88** 4987.

Belloni L, 1998, *Colloid Surf A* **140** 227.

Bloomfield V A, 1991, *Biopolymers* **31** 1471.

Borukhov I, Andelman D, and Orland H, 1997, *Phys Rev Lett* **79** 435.

Borukhov, I, Andelman D, and Orland H, 1998, *Eur Phys J B* **5** 869.

Borukhov I, Andelman D, and Orland H, 2000, *Electrochim. Acta* **46** 221.

Burak Y and Andelman D, 2000, *Phys Rev E* **62** 5296.

Burak Y and Andelman D, 2001, *J Chem Phys* **114** 3271.

Burak Y, Ariel G, and Andelman D, 2003, *Biophys J* **85** 2100.

Burak Y, Andelman D, and Orland H, 2004a, *Phys Rev E* **70** 016102.

Burak Y, 2004b, *Ph.D Thesis* (Tel Aviv University), unpublished.

Burak Y, Ariel G, and Andelman D, 2004c, *Curr Opin Colloid Interface Sci* **9** 53.

Chapman, D L, 1913, *Philos Mag* **25** 475.

Evans D F and Wennerström, H, 1994, *The Colloidal Domain*, (VCH Publishers, New-York).

Debye P and Hückel E, 1923, *Physik Z* **24** 185. An English translation is published in: *The collected works of Peter J W Debye*, 1954, (Interscience, New York).

De Gennes P G, 1979, *Scaling Concepts in Polymer Physics*, (Cornell Univ., Ithaca).

Deryagin B V and Landau L D, 1941, *Acta Physicochim URSS* **14** 633.

Deserno M, Arnold A, and Holm C, 2003, *Macromolecules* **36** 249.

Fisher M E, 1994, *J Stat Phys*, **75** 1, and references therein.

Fuoss R M, Katchalsky A, and Lifson S, 1951, *Proc Natl Acad Sci (USA)* **37** 579.

Le Bret M and Zimm B H, 1984, *Biopolymers* **23** 287.

Gelbart W M, Bruinsma R F, Pincus P A, and Parsegian V A, 2000, *Physics Today* **53** 38.

Gouy G, 1910, *J Phys (Paris)* **9** 457.

Gouy G, 1917, *Ann Phys* **7** 129.

Grahame D C, 1947, *Chem Rev* **41** 441.

- Grønbech-Jensen N, Mashl R J, Bruinsma R F, and Gelbart W M, 1997, *Phys Rev Lett* **78** 2477.
- Grosberg A Y, Nguyen T T, and Shklovskii B, 2002, *Rev Mod Phys* **74** 329.
- Guàrdia E, Rey and R, Padró A, 1991, *J Chem Phys* **95** 2823.
- Guldbrand L, Jönsson B, Wennerström H, and Linse P, 1984, *J Chem Phys* **80** 2221.
- Ha B Y and Liu A J, 1997, *Phys Rev Lett* **79** 1289.
- Hansen J P and McDonald I R, 1986, *Theory of Simple Liquids*, 2nd ed., (Academic Press, London).
- Henderson D, 1992, in *Fundamentals of Inhomogeneous Fluids*, D. Henderson (ed.), (Marcel Dekker, New York), Chap. 6, p. 177.
- Israelachvili J N, 1992, *Intermolecular and Surface Forces* (Academic Press, London).
- Kjellander R and Marčelja S, 1984, *Chem Phys Lett* **112** 49; 1985, **114** 124(E).
- Kjellander R and Marčelja S, 1985, *J Chem Phys* **82** 2122.
- Kjellander R, Åkesson T, Jönsson B, and Marčelja S, 1992, *J Chem Phys* **97** 1424.
- Kjellander R, 1996, *Ber Bun Phys Chem* **100** 894.
- Levin Y, 2002, *Rep Prog Phys* **65** 1577.
- Manning, G S, 1969, *J Chem Phys* **51** 924.
- Moreira A G and Netz R R, 2002, *Eur Phys J E* **8** 33.
- Netz R R and Andelman D, 2003, *Phys Rep* **380**, 1.
- Netz R R and Orland H, 2000, *Eur Phys J E* **1** 203.
- Neu J C, 1999, *Phys Rev Lett* **82** 1072.
- Odijk T, 1977, *J Polym Sci Part B: Polym Phys* **15** 477.
- Oosawa F, 1971, *Polyelectrolytes* (Marcel Dekker, New York).
- Parsegian V A and Gingell D, 1972, *Biophys J* **12** 1192.
- Pincus P A and Safran S A, 1998, *Europhys Lett* **42** (1998) 103.
- Podgornik R, 1990, *J Phys A* **23** 275.
- Ramanathan G V, 1986, *J Chem Phys* **85** 2957.
- Ramanathan G V, 1988, *J Chem Phys* **88** 3887.
- Raspaud E, de la Cruz M O, Sikorav J L, and Livolant F, 1998, *Biophys. J* **74** 381.
- Rau D C and Parsegian A, 1992a, *Biophys J* **61** 246.
- Rau D C and Parsegian A, 1992b, *Biophys J* **61** 260.
- Rosenfeld Y and Ashcroft NW, 1979, *Phys Rev A* **20** 1208.
- Sader J E and Chan D Y C, 1999, *J Coll Interface Sci* **213** 268.
- Sader J E and Chan D Y C, 2000, *Langmuir* **16** 324.
- Skolnick J and M. Fixman M, 1977, *Macromolecules* **10** 944.
- Tracy C A and Widom H, 1997, *Physica A* **244** 402.
- Verwey E J W and Overbeek J Th G, 1948, *Theory of the Stability of Lyophobic Colloids*, (Elsevier: New York).